

## Article

# Study of the Extraction Kinetics of Lithium by Leaching $\beta$ -Spodumene with Hydrofluoric Acid

Gustavo D. Rosales <sup>1</sup>, María C. Ruiz <sup>2</sup> and Mario H. Rodriguez <sup>1,\*</sup>

<sup>1</sup> Laboratorio de Metalurgia Extractiva y Síntesis de Materiales (MESiMat), Facultad de Ciencias Exactas y Naturales, Universidad Nacional de Cuyo, Mendoza 5500, Argentina; gd\_rosales@hotmail.com

<sup>2</sup> Instituto de Investigaciones en Tecnología Química (INTEQUI)-UNSL-CONICET, San Luis 5700, Argentina; mruiz@unsl.edu.ar

\* Correspondence: mrodriguez@uncu.edu.ar; Tel.: +54-9261-337-9329

Academic Editor: William Skinner

Received: 14 July 2016; Accepted: 20 September 2016; Published: 26 September 2016

**Abstract:** Parameters affecting the kinetics of the dissolution of  $\beta$ -spodumene with hydrofluoric acid have been investigated. The experimental tests were carried out in a closed vessel. The influence of several parameters, such as stirring speed, temperature, and reaction time were studied in order to deduce the kinetics of the dissolution reaction. The other parameters, particle size  $-45\ \mu\text{m}$ ; HF concentration 4%  $v/v$ , and the solid–liquid ratio 0.95%  $w/v$  were kept constant. The results indicate that the stirring speed does not have an important effect on the dissolution of the mineral above 330 rpm. The extent of the leaching of  $\beta$ -spodumene increases with temperature and reaction time augmentations. Scanning electron microscope (SEM) analyses of some residues in which the conversion was lower than 30% indicated a selective attack on certain zones of the particle. The treatment of the experimental data was carried out using the Modelado software. The model that best represents the dissolution of the mineral is the following:  $\ln(1 - X) = -b_1 [\ln(1 + b_2t) - b_2t/(1 + b_2t)]$ . This model is based on “nucleation and growth of nuclei” theory, and describes the style of attack physically observed by SEM on the residues.

**Keywords:** lithium; leaching; kinetics; hydrofluoric acid

## 1. Introduction

The production and economic benefit of every metal extraction process is directly related to the rate of the chemical reactions that take part in it. In hydrometallurgical processes, working temperatures are lower than those used in pyrometallurgical processes, which implies lower reaction rates and that the limitations found in these processes are mainly kinetic. Because of this, it is of particular importance to know the kinetic models and the mechanisms involved in the leaching process, which explain how the dissolution reaction occurs for extraction of Li.

Lithium is considered a strategic metal whose use has significantly expanded in the last years. Lithium compounds are used in the preparation of lubricants, in the manufacture of glass and special alloys, and also in the pharmaceutical industry, in the production of drugs used in psychiatry. One of the most important uses of Li and its compounds is in the manufacture of energy storage cells for electronic devices and hybrid or electric cars [1–3].

Lithium is found in many minerals due to its high chemical reactivity. However, there are few minerals that have been used for the production of lithium compounds. The most important lithium mineral is spodumene, which generally is accompanied by quartz, feldspar, and mica [2,4]. Spodumene occurs naturally in  $\alpha$  phase, with a monoclinic structure of the pyroxene type. This structure is resistant to the attack of chemical agents, either gaseous or liquid. Spodumene transforms into its  $\beta$ -phase through calcination at 1373 K; this phase is much more reactive and less resistant to ordinary chemical

agents. The most common industrial processes for the extraction of lithium from spodumene are acid and alkaline digestion, and the ion exchange method. The products obtained through these methods are lithium carbonate, lithium hydroxide, and lithium chloride, respectively. Acid digestion is carried out with concentrated sulfuric acid at temperatures higher than 523 K, whereas alkaline digestion is carried out with  $\text{CaCO}_3$  at 1313 K. In the process of ion exchange,  $\beta$ -spodumene is heated with organic salts of sodium and potassium at 673 K [2,4]. The sulfuric acid process has become the main method for the production of lithium carbonate from spodumene due to its high efficiency. However, these methods have intrinsic drawbacks, such as high levels of sulfate and heavy metal ions in the product, sophisticated process for recovering sodium sulfate, and high energy consumption [3,4]. Furthermore, in the sulfuric process, 0.95 tons of acid residue are generated for each ton of processed mineral; this indicates that only Li is recovered from  $\beta$ -spodumene, and Al and Si remain as waste.

There have been published relevant findings about the dissolution of  $\beta$ -spodumene in an autoclave at temperatures around 523 K with salts such as  $\text{Na}_2\text{CO}_3$  and  $\text{NaCl}$  [5]. Other recently used routes are the pyrometallurgical chlorination of  $\beta$ -spodumene with  $\text{Cl}_{2(g)}$  or by calcination with  $\text{CaCl}_{2(s)}$  at temperatures between 1173 and 1373 K [6,7].

Rosales et al. investigated the leaching process of  $\beta$ -spodumene in hydrofluoric acid medium. They found that the optimal conditions to achieve a lithium extraction higher than 90% were: solid–liquid ratio, 1.82% ( $w/v$ ); temperature, 348 K; HF concentration, 7% ( $v/v$ ), and reaction time, 10 min. Furthermore, they proposed the following dissolution reaction [7,8]:



Then, Li, Al, and Si can be recovered as  $\text{Li}_2\text{CO}_3$ ,  $\text{Na}_3\text{AlF}_6$ , and  $\text{Na}_2\text{SiF}_6$ , respectively. This process has the advantage that it can be performed at low leaching temperature (<348 K), low HF concentration, and it uses all the elemental components present in the mineral. The lithium recovery efficiency achieved in the process reaches 90%.

There have been published relevant findings about the dissolution kinetics of aluminosilicates (kaolins and feldspars) with HF. Kline and Fogler reported the probable mechanisms by which the dissolution reaction of some aluminosilicates takes place, proposing that the dissolution products are fluorosilicates and fluoroaluminates ( $\text{SiF}_m^{4-m}$  and  $\text{AlF}_n^{3-n}$ , where  $m$  and  $n$ : 1, 2, ..., 6) of great stability. Moreover, these authors conclude that the rate of dissolution is controlled by the adsorption of HF molecules on the surface of the silicates. The dissolution was catalyzed by strong acids or salts, due to the adsorption of cations or protons over the hydroxyls of the surface of the structure [9,10]. Kumar et al. suggested that the dissolution of the aluminosilicates with HF is accompanied by the appearance of fluorinated acid complexes of Al and Si:  $\text{H}_3\text{AlF}_6$  and  $\text{H}_2\text{SiF}_6$ , respectively [11,12].

Therefore, the aim of this study was to present a kinetic study of the dissolution of  $\beta$ -spodumene with HF. This study explains the kinetics and the way in which the dissolution reaction occurs (nature, rate, and dependence of the reaction on variables such as time, temperature, and stirring speed). Along with the chemical kinetics, we determined a mathematical model that yields a good approximation of the way HF behaves when it reacts with the mineral.

## 2. Materials and Methods

The leaching agent was HF, 40%  $w/w$ , analytical grade. The mineral used was  $\alpha$ -spodumene, extracted from the mine “Las Cuevas”, located in the department of San Martín, San Luis, Argentina. The  $\alpha$ -spodumene sample was calcined from room temperature to 1373 K in an electric furnace with a heating rate of 10 K/min in order to transform it into its  $\beta$ -phase, which is more susceptible to acid dissolution [1,3]. Characterization of the ore was performed by X-ray fluorescence (XRF) on a Philips PW 1400 instrument (Philips, Amsterdam, The Netherlands) and by X-ray diffraction (XRD) on a Rigaku D-Max III C diffractometer (Rigaku, Osaka, Japan), operated at 35 kV and 30 mA. The  $\text{K}\alpha$  radiation of Cu and a filter of Ni,  $\lambda = 0.15418$  nm were used. Morphological

analysis was done by scanning electron microscope (SEM) in a LEO 1450 VP (Zeiss, Jena, Germany) which was equipped with an X-ray dispersive spectrometer EDAX, Genesis 2000, used to determine semi-quantitative composition of the residues obtained through the leaching of the minerals by electron probe microanalysis (EPMA).

Determination of lithium content in the ore was performed by atomic absorption spectroscopy (AAS) using a Varian SpectrAA 55 spectrometer (Palo Alto, CA, USA) with a hollow-cathode lamp (analytical error 1.5%). Previously, the sample ( $\alpha$ -spodumene) was dissolved using a concentrated mixture of sulfuric acid and hydrofluoric acid according to the method of Brumbaugh and Fanus [13]. The bulk composition of the ore is shown in Table 1, as determined by AAS (Li and Na) and XRF (Si, Al, Fe, Ca, Mg, K, and Ti).

**Table 1.** The bulk composition of the ore.

Component	% w/w
SiO <sub>2</sub>	68.3
Al <sub>2</sub> O <sub>3</sub>	18.6
Fe <sub>2</sub> O <sub>3</sub>	3.21
CaO	0.52
MgO	0.29
K <sub>2</sub> O	0.14
Na <sub>2</sub> O	0.78
Li <sub>2</sub> O	7.03
TiO	0.11
Others	0.12

The results of the characterization of the ore by XRD are shown in Figure 1.

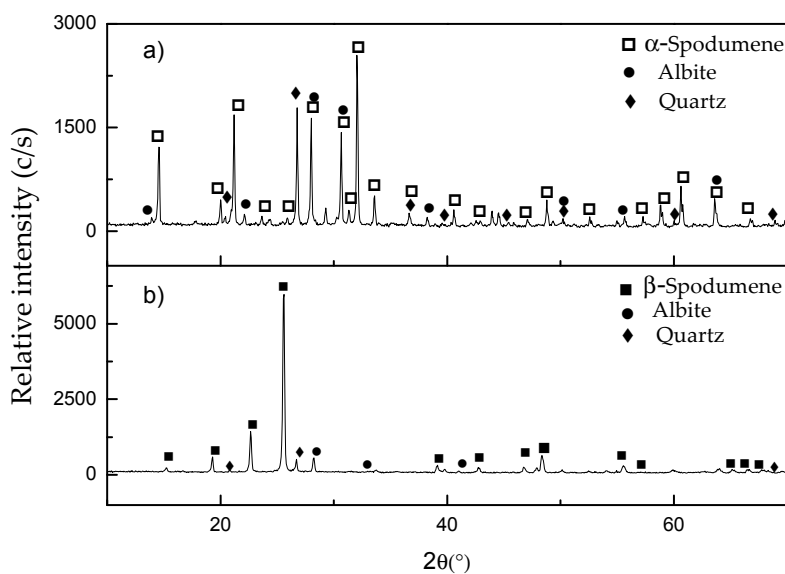


**Figure 1.** Diffractograms of the mineral: (a)  $\alpha$ -spodumene and (b)  $\beta$ -spodumene.

In Figure 1a, XRD patterns show that the sample is mainly composed of  $\alpha$ -spodumene (Joint Committee on Powder Diffraction Standards—JCPDS 33-786), with the presence of albite (International Centre for Diffraction Data—ICDD 96-900-1631) and quartz (JCPDS 33-1161) as gangue. The diffractogram in Figure 1b shows the appearance of  $\beta$ -spodumene (JCPDS 35-797) after thermal treatment of the ore. The  $\alpha$ -phase is not detected, indicating that the transformation of  $\alpha$ -phase to  $\beta$ -phase was complete. Albite and quartz were also detected. The quartz content in sample (b)

(8%  $w/w$ ) was determined by XRD, using the standard addition method, diffraction line 26.7 degrees of  $\text{SiO}_2$  as standard [8].

In Figures 2 and 3, the results of the characterization of the mineral by SEM are shown.

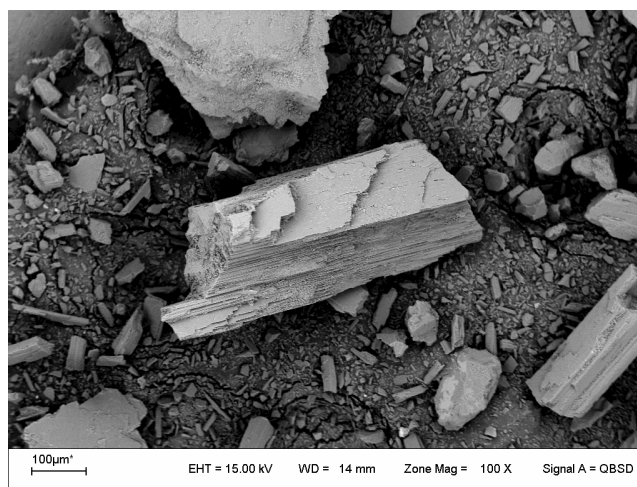


**Figure 2.** SEM micrograph of the mineral without thermal treatment ( $\alpha$ -spodumene).

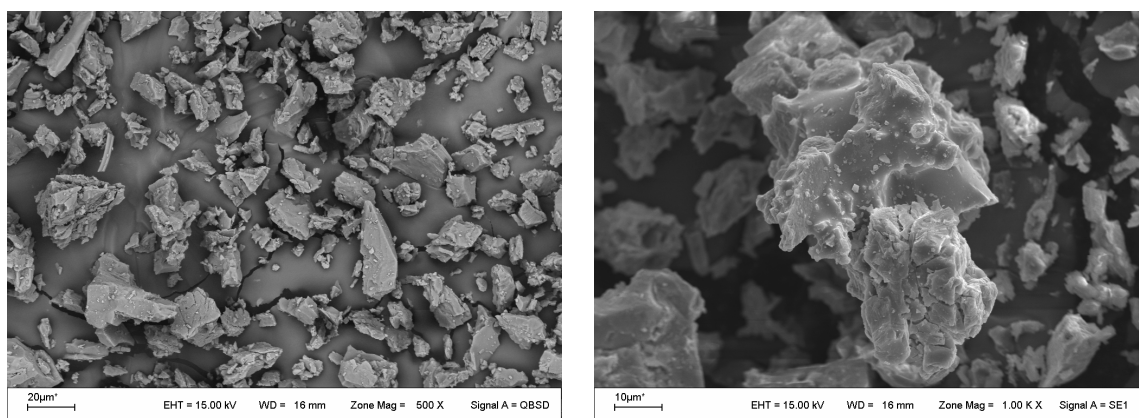


**Figure 3.** SEM micrograph of the mineral with thermal treatment ( $\beta$ -spodumene).

In Figure 2, the micrograph corresponding to the mineral in its  $\alpha$  phase is presented. It can be observed that the particles of the mineral without thermal treatment exhibit an irregular shape and a prismatic structure with a flattened elongated habit, which agrees with that reported in the bibliography [2,14].

Figure 3 shows the results of the SEM characterization of the mineral with thermal treatment.

In these micrographs, it can be observed that  $\beta$ -spodumene particles are different from the  $\alpha$ -spodumene in their morphology, since no prismatic structures are observed in the  $\beta$ -phase particles. When the  $\alpha$ -structure has transformed into the new  $\beta$ -spodumene structure, the increasing stress due to the volumetric expansion leads to the breakdown of the original particles, and therefore to a particle size reduction. This is caused by the thermal treatment of the sample [14].

The specific surface area of the  $\beta$ -spodumene was determined by Brunauer–Emmett–Teller (BET) with  $\text{N}_2$  adsorption at 77 K in a Micromeritics Gemini V (Micromeritics, Norcross, GA, USA). The BET analysis showed a low specific area ( $1.41 \text{ m}^2/\text{g}$ ), indicating a low porosity of  $\beta$ -spodumene grains.

### Experimental Equipment and Procedure

The experimental tests were performed in a closed 500 mL PVC vessel equipped with magnetic stirring and temperature control systems.

To perform each test, 3 g of ore and 300 mL of distilled water were placed into the reactor. This mixture was heated with stirring until the work temperature was reached. Then, 12 mL of HF (leaching agent) was added, and at that moment, reaction time began to be measured. Once the experiment was finished, the solid was filtered, dried at 348 K, and then weighed. All the experiments were performed in triplicate.

The course of the dissolution reaction was followed by Equation (2):

$$X = (m_i - m_f)/m_i \quad (2)$$

where  $X$  is the conversion,  $m_i$  is the initial mass of the mineral and  $m_f$  is the final mass of the residue after the leaching.

## 3. Results

### 3.1. Effect of Stirring Speed

To study the effect of stirring speed on the conversion of the mineral, the experiments were performed in conditions of solid–liquid ratio, 0.96% ( $w/v$ ); reaction time, 30 min; HF concentration, 4% ( $v/v$ ); and temperature, 298 K. The experimental results are shown in Figure 4.

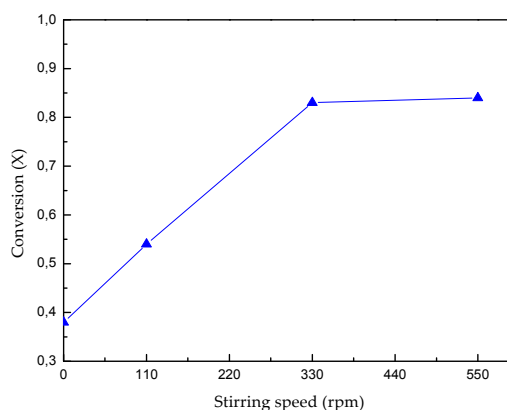


**Figure 4.** Effect of stirring speed on the dissolution of the mineral.

Figure 4 illustrates that stirring speed has an obvious effect on the leaching process. When the stirring speed is over 330 rpm, the mineral conversion remains constant. This fact indicates that once this stirring speed is reached, the thickness of the film surrounding the solid is minimal, and hence when it is over 330 rpm, it does not affect HF transference rate from the solution to the particle surface.

### 3.2. Effect of Temperature and Reaction Time

The effect of the temperature and the reaction time on  $\beta$ -spodumene dissolution was studied between 278 and 308 K during 1 to 30 min, respectively. The results are presented in Figure 5.

The results show that the extent of leaching increases with the temperature and the reaction time, reaching a mineral dissolution of 88% in 30 min at 308 K. It can be observed that for reaction temperatures of 298 and 308 K, as reaction time increases after 10 min, the extraction efficiency remains almost constant.



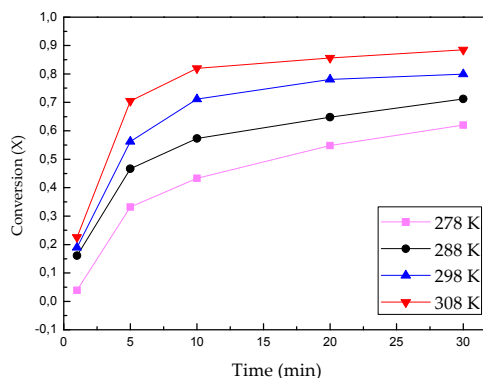


**Figure 5.** Effect of reaction time and temperature on the dissolution of the mineral.

### 3.3. Characterization of the Leaching Residues

In order to understand the type of chemical attack, residues from tests were analyzed by XRD, SEM, and EPMA. The results are shown in Figures 6–8, respectively.

It can be inferred from Figure 6 that a partial dissolution of  $\beta$ -spodumene is achieved. The diffractogram shows an enhancement in the intensities of the peaks corresponding to quartz and albite structures; this indicates that the dissolution reaction occurs only over  $\beta$ -spodumene [7,8]. Other new structures are not observed in the leaching residue.

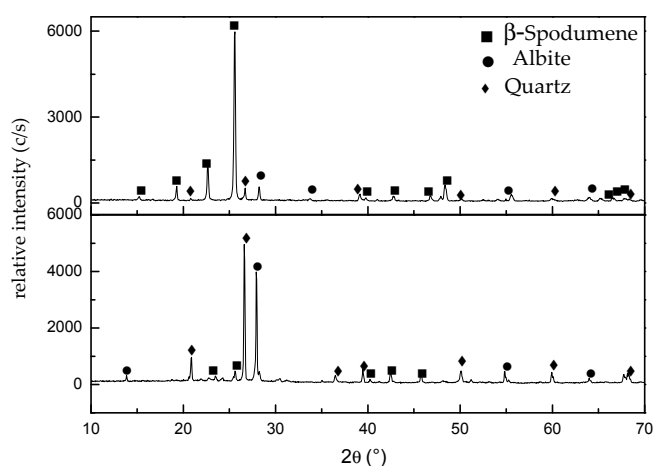


**Figure 6.** XRD of the leaching residues (X: 0.2; time: 1 min; and temperature: 308 K).

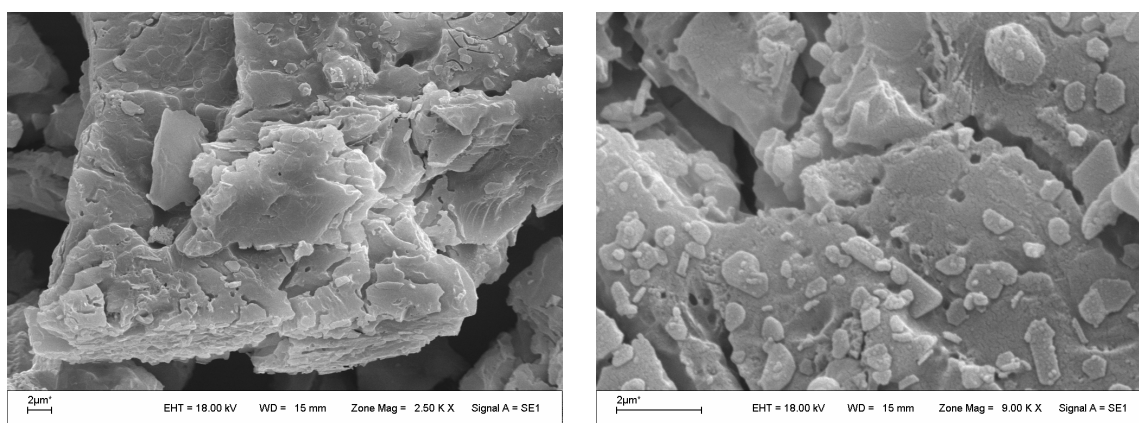


**Figure 7.** SEM micrographs of the leaching residue (X: 0.04; time: 1 min; and temperature: 278 K).

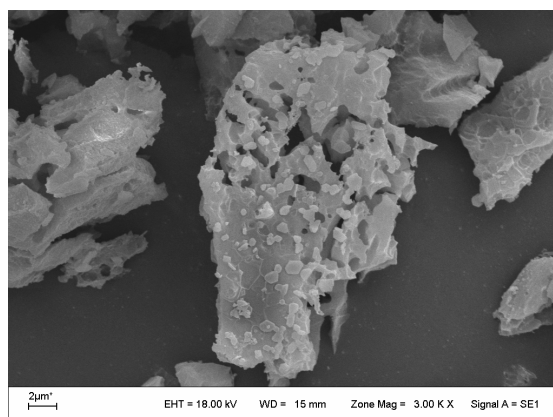


**Figure 8.** SEM micrographs of the leaching residue (X: 0.2; time: 1 min; and temperature: 308 K).

Figure 7 shows a micrograph of a particle corresponding to a sample dissolved at 298 K for a period of 1 min, from which small holes on its surface can be seen. This indicates that a selective attack is produced on  $\beta$ -spodumene in preferential sites of the particle. Figure 8 shows a residue obtained for 1 min at 308 K with a conversion of 0.2; it can be noted from this figure that the original small holes have grown to a great extent.

The EPMA analysis conducted on leaching residues at different temperatures shows only the presence of the elements O, Al, and Si in the proportions shown in Table 2. These results, along with the ones obtained by XRD suggest that there is no accumulation of impurities or the formation of new compounds during leaching.

**Table 2.** EPMA analysis, in at %, corresponding to leaching residues obtained at different temperatures.

Temperature (K)	% O	% Al	% Si	% F
278	32	17	51	-
288	40	16	43	-
298	37	16	46	-
308	48	12	39	-

### 3.4. Kinetic Model

The experimental data of the mineral dissolution in HF medium were analyzed with the Modelado software developed by Quiroga (2002). This software was designed for the kinetic treatment of different types of heterogeneous reactions, such as sublimation of solids in gases, catalytic, and non-catalytic solid–fluid reactions [15–18]. The kinetic model was estimated using the experimental data obtained at different temperatures (Figure 5), selecting as most probable models those that had regression errors—associated with each temperature level—less than 5%. Moreover, the hypotheses of each model formulation and the results obtained from the characterization of the leaching residues (XRD, SEM, and EPMA) were taken into consideration.

The model of “sequential nucleation and growth” best fitted the experimental data of  $\beta$ -spodumene dissolution at different temperatures. The mathematical expression of this model is the following:

$$\ln(1 - X) = -b_1 \left[ \ln(1 + b_2 t) - \frac{b_2 t}{1 + b_2 t} \right] \quad (3)$$

where  $b_1$  and  $b_2$  coefficients are defined as:

$$b_1 = \frac{\sigma_g N_S^0 \Omega^0 b M_B r_S}{b_2 \rho d_p} \quad (4)$$

$$b_2 = k_{N_2} N_S^0 \quad (5)$$

In Equations (4) and (5),  $r_S$ ,  $k$ , and  $k_{N_2}$  are defined as:

$$r_S = k c_A^n \quad k = A_1 e^{-\frac{E_a}{RT}} \quad k_{N_2} = A_2 e^{-\frac{E_N}{RT}} \quad (6)$$

where  $k$  and  $k_{N_2}$  are the kinetic coefficients of the reaction rate and the formation rate of the sites, respectively;  $A$  is the frequency factor;  $E_a$  and  $E_N$  are the apparent activation energy and energy of the nucleation, respectively;  $R$  is the gas constant; and  $T$  is the temperature. The values of the kinetic parameters estimated by the software are shown in Table 3. The kinetic constant  $k$  is defined as the product between  $b_1$  and  $b_2$  [19].

**Table 3.** Kinetic parameters of the estimated model.

Temperature (K)	$b_1$	$b_2$	$k$
278	0.3698	1.116	0.4126
288	0.3812	2.257	0.8603
298	0.5020	2.580	1.295
308	0.5346	5.355	2.862

The results of experimental data adjustment ( $X$  vs.  $t$  at different temperatures) with the model are shown in Figure 9. It can be noted that the experimental results and the values predicted by the kinetic model are in excellent agreement, as can be seen from the values of the squared correlation coefficient,  $R^2$ .

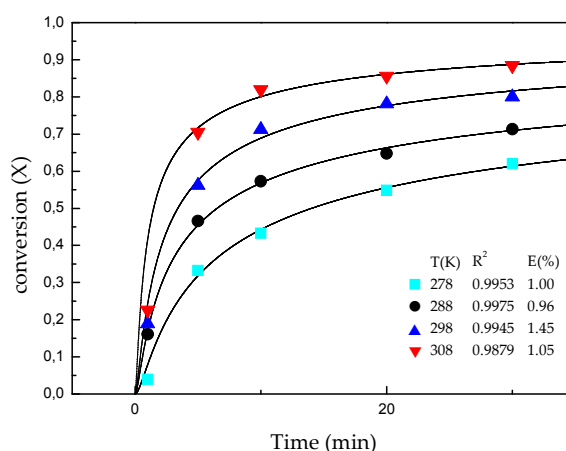


**Figure 9.** Correlation between experimental data and the proposed model.

The proposed kinetic model is based on the “nucleation and growth of nuclei” theory, which was originally developed for the modeling of transformation reactions and solid decomposition [20]. Delmon adapted this theory to fluid–solid reactions, changing the concept of “nucleation” and the “growth of nuclei” to “activation in active sites” and “growth of holes”, respectively [21].

The selected model proposes a sequential nucleation process where the reactant particle is constituted by a pure non-porous solid reagent, and there is no formation of solids that remain attached to the particle [19]. These hypotheses are consistent with the results obtained by BET, XRD, SEM, and EPMA.

The model presumes a system where the solid reagent undergoes a topochemical-type attack in specific sites of the particle surfaces. The causes of the origin of preferential sites of interaction can be diverse, such as heterogeneities often present in solid surfaces caused by crystal defects or impurities in the solid [19]. The reaction starts in these preferential points susceptible to chemical interaction and



then progresses, a fact manifested by the formation of holes that grow from the surface towards the interior of the particle. The results obtained by SEM performed on the residues of the mineral samples dissolved in HF medium (Figures 7 and 8) allow us to confirm that the experimental data coincide with the hypothesis from the model. Barbosa et al. studied the kinetics of  $\beta$ -spodumene chlorination, and found that the reaction with chlorine begins in preferential sites of the mineral surface. They suggest that the defects contained in the crystal structure of the mineral may account for the formation of these preferential sites [16].

#### 3.4.1. Process Controlling Stage

Habashi proposed that the rate-controlling stage of the reaction can be determined through the value of the apparent activation energy ( $E_a$ ) of such a reaction. A diffusion-controlled process is characterized by being slightly dependent on temperature, while the chemically controlled process is strongly dependent on temperature. Therefore, the diffusion and rate coefficients depend linearly and exponentially on temperature, respectively. In Table 4, the different kinds of control are shown, according to the value of  $E_a$  [22].

**Table 4.** Control according to the  $E_a$  value.

$E_a$ (kJ/mol)	Control
<12.5	Diffusional
21–33.5	Intermediate
>41.8	Chemical

The value of the kinetic coefficient of the reaction rate was calculated using Equation (6). The  $E_a$  value of the dissolution reaction was calculated from a plot of  $\ln k$  vs.  $1/T$ , and these results are shown in Figure 10.

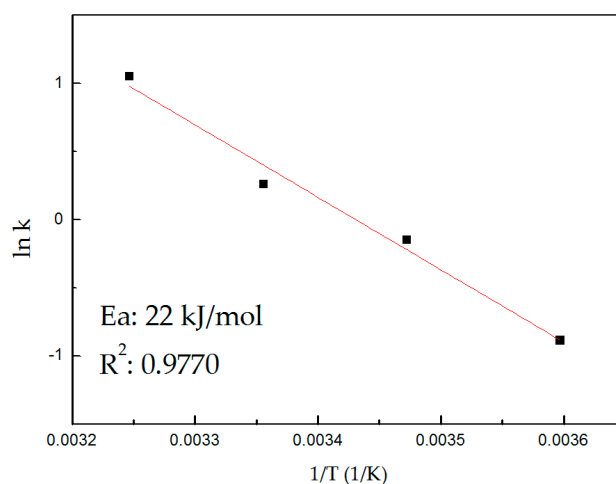


**Figure 10.** Arrhenius plot for the  $\beta$ -spodumene dissolution in HF medium.

The slope of Figure 10 allows us to estimate the apparent activation energy for the  $\beta$ -spodumene dissolution, being  $E_a = 22$  kJ/mol. From the  $E_a$  value, it can be suggested that the leaching process is controlled by two stages, the formation of the reaction interface (diffusional control) and the chemical reaction (chemical control) [15,16].

### 3.4.2. Reaction Mechanism

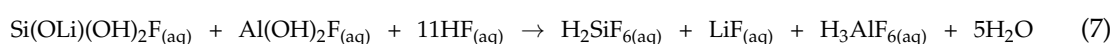
Based on the bibliography and the experimental data presented in this study, it is proposed that the global rate of the dissolution process of the mineral is controlled by the stages of adsorption of the fluid reagent and chemical reaction, according to the following mechanism:

#### (a) First stage (adsorption of the fluid reagent)

This stage begins with the chemical adsorption of HF molecules over the mineral surface, precisely over Si and Al atoms, which are hydrolyzed in acidic media. When HF molecules are adsorbed at the mineral surface, the surface bonds are further weakened by the association of the HF protons with the adjacent lattice oxygens. Consequently, the reactive intermediate is a surface site at which the lattice atoms are partially bonded to each other and partially to hydrogen and fluorine [9,10]. In this stage, the intermediates  $\text{Al}(\text{OH})_2\text{F}$  and  $\text{SiOLi}(\text{OH})_2\text{F}$  are formed [23].

#### (b) Second stage (chemical reaction)

In the second stage, the formed intermediates react with other HF molecules, forming  $\text{H}_2\text{SiF}_6$  and  $\text{H}_3\text{AlF}_6$  (Equation 7). These acid complexes diffuse to the bulk solution, leaving holes or reaction nuclei, from which the dissolution reaction continues.



Kline and Fogler proposed a similar mechanism for the dissolution of other aluminosilicates with HF, assuming that HF reacts with the atoms of the surface of the mineral that are hydrolyzed to form the compounds  $\text{Al}(\text{OH})\text{F}^-$  and  $\text{Si}(\text{OH})\text{F}^{-2}$  [9,10]. They concluded that the dissolution of silicates with hydrofluoric acid can be attributed to the fact that adsorption of the attacking species increases the coordination of the surface silicon and aluminum, thus weakening the lattice bonds.

## 4. Conclusions

The extraction of lithium through the leaching of  $\beta$ -spodumene with HF is highly dependent on the temperature and reaction time. The stirring speed does not have an important effect on the dissolution of the mineral above 330 rpm. The maximum dissolution of the mineral (88%) is reached in 30 min with 4% *v/v* HF acid at 308 K with a stirring speed of 330 rpm.

The SEM characterization of the leaching residues indicates that  $\beta$ -spodumene undergoes an irregular located-type attack in preferential sites of the particle, where the reaction develops.

The model based on “nucleation and nuclei growth”, represented by Equation (3), best fits the experimental results of the mineral dissolution in HF media. Moreover, the characterization of the residues physically supports the hypothesis formulated in the kinetic model.

The determined apparent activation energy was 22 kJ/mol in the temperature range of 278–308 K. This  $E_a$  value would suggest that the leaching process is controlled by two stages, the formation of the reaction interface (diffusional control) and the chemical reaction (chemical control).

**Acknowledgments:** The financial support from Universidad Nacional de Cuyo, Secretaria de Ciencia, Técnica y Posgrado, is gratefully acknowledged. Three anonymous referees provided constructive and helpful reviews, corrections and comments. Many thanks are due to the Editorial staff of Minerals.

**Author Contributions:** Gustavo D. Rosales, María C. Ruiz and Mario H. Rodríguez conceived and designed the experiments; Gustavo D. Rosales and Mario H. Rodríguez performed the experiments and analyzed the data; María C. Ruiz and Mario H. Rodríguez contributed with reagents, materials and analysis tools; Gustavo D. Rosales and Mario H. Rodríguez wrote the paper.

**Conflicts of Interest:** The authors declare no conflict of interest.

## Appendix A

### Symbols

$b$	Stoichiometric coefficient
$b_1$ and $b_2$	Coefficients defined by Equations (4) and (5), respectively
$C_A$	Concentration of HF evaluated on the interface of reaction, mol/L
$d_p^0$	Initial particle diameter, mm
$E_a$	Activation energy, kJ/mol
$k$	Kinetic coefficient of the reaction rate, m/s
$k_{N_2}$	Kinetic coefficient of the formation of the sites, m <sup>2</sup> /s
$MB$	Molecular weight of the solid reactant, g/mol
$N_E^0$	Number of moles per surface unit of a chemical specie E
$N_S^0$	Initial number of the sites than can be activated per unit of initial surface of the particle
$N_S$	Number of the active sites per surface unit
$p$	Growth factor
$R$	Gas constant, kJ/mol K
$r_S$	Reaction solid–fluid rate, mol/cm <sup>2</sup> min
$T$	Temperature, K
$t$	Time, min
$X$	Solid conversion

### Greek Symbols

$\rho$	Solid density, kg/m <sup>3</sup> .
$\Omega_0$	Initial particle surface, m <sup>2</sup> .
$\sigma_g$	Coefficient of shape of the hole.

### References

- Garret, D.E. Part 1—Lithium. In *Handbook of Lithium and Natural Calcium Chloride*; Elsevier Ltd.: London, UK, 2004.
- Siame, E.; Pascoe, R.D. Extraction of lithium from micaceous waste from China clay production. *Min. Eng.* **2011**, *24*, 1595–1602. [[CrossRef](#)]
- Habashi, F. Alkali Metals-Lithium. In *Handbook of Extractive Metallurgy*; Wiley-VCH: Weinheim, Germany, 1997; Volume IV.
- Chen, Y.; Tian, Q.; Chen, B.; Shi, X.; Liao, T. Preparation of lithium carbonate from  $\beta$ -spodumene by a sodium carbonate autoclave process. *Hydrometallurgy* **2011**, *109*, 43–46. [[CrossRef](#)]
- Barbosa, L.; Valente, G.; Orosco, R.P.; Gonzalez, J.A. Lithium extraction from  $\beta$ -spodumene through chlorination with chlorine gas. *Min. Eng.* **2014**, *56*, 29–34. [[CrossRef](#)]
- Barbosa, L.; Ruiz, M.C.; Gonzalez, J.A. Extraction of lithium from  $\beta$ -spodumene using chlorination roasting with calcium chloride. *Thermochim. Acta* **2015**, *605*, 63–67. [[CrossRef](#)]
- Rosales, G.; Ruiz, M.C.; Rodriguez, M. Alkaline metal fluorides synthesis as subproduct of  $\beta$ -spodumene leaching. *Hydrometallurgy* **2013**, *139*, 73–78. [[CrossRef](#)]
- Rosales, G.; Ruiz, M.C.; Rodriguez, M. Novel process for the extraction of lithium from  $\beta$ -spodumene by leaching with HF. *Hydrometallurgy* **2014**, *147–148*, 1–6. [[CrossRef](#)]
- Kline, E.; Fogler, S. Dissolution kinetics: The nature of the particle attack of layered silicates in HF. *Chem. Eng. Sci.* **1980**, *36*, 871–884. [[CrossRef](#)]
- Kline, E.; Fogler, S. Dissolution kinetics: Catalysis by salts. *J. Colloid Interface Sci.* **1981**, *82*, 103–115. [[CrossRef](#)]
- Kumar, M.; Mankhand, T.R.; Murthy, D.S.R.; Mukhopadhyay, R.; Prasad, P.M. Refining of a low-grade molybdenite concentrate. *Hydrometallurgy* **2006**, *86*, 56–62. [[CrossRef](#)]
- Kumar, M.; Nani, M.; Mankhand, T.; Pandey, B. Precipitation of sodium silicofluoride (Na<sub>2</sub>SiF<sub>6</sub>) and cryolite (Na<sub>3</sub>AlF<sub>6</sub>) from HF/HCl leach liquors of alumino-silicates. *Hydrometallurgy* **2010**, *104*, 304–307. [[CrossRef](#)]

13. Brumbaugh, R.; Fanus, W. Determination of lithium in spodumene by flame photometry. *Anal. Chem.* **1954**, *26*, 463–465. [[CrossRef](#)]
14. Salakjani, N.; Singh, P.; Nikoloski, A.N. Mineralogical transformations of spodumene concentrate from Greenbushes, Western Australia. Part 1: Conventional heating. *Min. Eng.* **2016**, *98*, 71–79. [[CrossRef](#)]
15. Quiroga, O.D.; Avanza, J.R.; Fusco, A.J. *Modelado Cinético de las Transformaciones Fluido-Sólido Reactivo*; Editorial Universitaria de la Universidad del Nordeste (EUDENE): Buenos Aires, Argentina, 1996. (In Spanish)
16. Barbosa, L.; Valente, G.; Gonzalez, J.A. Kinetic study on the chlorination of  $\beta$ -spodumene for lithium extraction with  $\text{Cl}_2$  gas. *Thermochim. Acta* **2014**, *557*, 61–67. [[CrossRef](#)]
17. Tunez, F.; Orosco, P.; Gonzalez, J.A.; Ruiz, M.C. Kinetic study on the chlorination of indium oxide. *Thermochim. Acta* **2011**, *524*, 151–156. [[CrossRef](#)]
18. Rodriguez, M.; Quiroga, O.; Ruiz, M.C. Kinetic study of ferrocolumbite dissolution in hydrofluoric acid medium. *Hydrometallurgy* **2007**, *85*, 87–94. [[CrossRef](#)]
19. Quiroga, O.D. Modelado. In *Software para el Tratamiento Cinético de Transformaciones Fluido Sólido-Reactivo*; INIQUI (UNSa-CONICET): Salta, Argentina, 2002. (In Spanish)
20. Delmon, B. *Introduction a la Cinétique Hétérogène*; Editions Technip: Paris, France, 1969. (In French)
21. Avrami, M. Kinetic of phase change. I General theory. *J. Chem. Phys.* **1963**, *7*, 1103. [[CrossRef](#)]
22. Habashi, F. *Principles of Extractive Metallurgy*; Gordon and Breach: New York, NY, USA, 1980; Volume I.
23. Fernández Lisboa, D.; Steel, M.K. Recovery of fluoride values from spent pot-lining: Precipitation of an aluminum hydroxyfluoride hydrate product. *Sep. Purif. Technol.* **2008**, *61*, 182–192. [[CrossRef](#)]



© 2016 by the authors; licensee MDPI, Basel, Switzerland. This article is an open access article distributed under the terms and conditions of the Creative Commons Attribution (CC-BY) license (<http://creativecommons.org/licenses/by/4.0/>).